

Synthesis, Characterization, and Hydrolysis Products of $(\eta^2\text{-}t\text{Bu}_2\text{pz})\text{AlH}(\mu:\eta^1,\eta^1\text{-}t\text{Bu}_2\text{pz})_2\text{AlH}_2$ – Structural Characterization of a Complex Containing η^1 -, η^2 -, and $\mu:\eta^1,\eta^1$ -Pyrazolato Ligands and a Complex Containing a Terminal Hydroxo Ligand

Zhengkun Yu,^{[a]†} John E. Knox,^[a] Andrey V. Korolev,^{[a]‡} Mary Jane Heeg,^[a]
H. Bernhard Schlegel,^[a] and Charles H. Winter*^[a]

Keywords: Hydrogen bond / N ligands / Aluminum / Pyrazolato ligands / Molecular orbital calculations

Treatment of alane–ethyltrimethylamine with 3,5-di-*tert*-butylpyrazole ($t\text{Bu}_2\text{pzH}$) in a 2:3 molar ratio afforded $[(\eta^2\text{-}t\text{Bu}_2\text{pz})\text{AlH}(\mu:\eta^1,\eta^1\text{-}t\text{Bu}_2\text{pz})_2\text{AlH}_2]$ in 57% yield. Hydrolysis of $[(\eta^2\text{-}t\text{Bu}_2\text{pz})\text{AlH}(\mu:\eta^1,\eta^1\text{-}t\text{Bu}_2\text{pz})_2\text{AlH}_2]$ afforded variable mixtures of $\text{Al}(t\text{Bu}_2\text{pz})_3$, $[(\eta^2\text{-}t\text{Bu}_2\text{pz})\text{AlH}(\mu:\eta^1,\eta^1\text{-}t\text{Bu}_2\text{pz})_2\text{AlH}(\text{OH})]$, and $[(\eta^2\text{-}t\text{Bu}_2\text{pz})\text{AlH}(\mu:\eta^1,\eta^1\text{-}t\text{Bu}_2\text{pz})_2\text{AlH}(\eta^1\text{-}t\text{Bu}_2\text{pz})]$. The structures of all new complexes were assigned from spectral and analytical data. In addition, the X-ray crystal structures of $[(\eta^2\text{-}t\text{Bu}_2\text{pz})\text{AlH}(\mu:\eta^1,\eta^1\text{-}t\text{Bu}_2\text{pz})_2\text{AlH}(\text{OH})]$ and $[(\eta^2\text{-}t\text{Bu}_2\text{pz})\text{AlH}(\mu:\eta^1,\eta^1\text{-}t\text{Bu}_2\text{pz})_2\text{AlH}(\eta^1\text{-}t\text{Bu}_2\text{pz})]$ were determined. $[(\eta^2\text{-}t\text{Bu}_2\text{pz})\text{AlH}(\mu:\eta^1,\eta^1\text{-}t\text{Bu}_2\text{pz})_2\text{AlH}(\text{OH})]$ crystallizes as a dimeric molecule, and contains two bridging pyrazolato ligands, one η^2 -pyrazolato ligand, as well as terminal hydrido and hydroxo ligands. The hydroxo and η^2 -pyrazolato ligands possess a syn-relationship within the dimer. The hydroxy group proton does not participate in dihydrogen bonding, and instead appears to be intramolecularly hydrogen-

bonded to the π -cloud of the η^2 -pyrazolato ligand. The overall structure of $[(\eta^2\text{-}t\text{Bu}_2\text{pz})\text{AlH}(\mu:\eta^1,\eta^1\text{-}t\text{Bu}_2\text{pz})_2\text{AlH}(\eta^1\text{-}t\text{Bu}_2\text{pz})]$ is very similar to that of $[(\eta^2\text{-}t\text{Bu}_2\text{pz})\text{AlH}(\mu:\eta^1,\eta^1\text{-}t\text{Bu}_2\text{pz})_2\text{AlH}(\text{OH})]$, except that the η^1 - and η^2 -pyrazolato ligands have an anti-disposition within the dimer. Molecular orbital calculations were carried out on $[(\eta^2\text{-}t\text{Bu}_2\text{pz})\text{AlH}(\mu:\eta^1,\eta^1\text{-}t\text{Bu}_2\text{pz})_2\text{AlH}(\text{OH})]$ to understand the hydrogen bonding and the η^2 -pyrazolato ligand coordination. The calculations predict that there is a 1.4 kcal/mol energy difference between η^1 - and η^2 -pyrazolato ligand coordination, which implies that the observed η^2 -pyrazolato ligand occurs due to accommodation of the bulky *tert*-butyl groups. The intramolecular hydrogen bond between the hydroxo ligand proton and the π -cloud of the η^2 -pyrazolato ligand is estimated to have a bond strength of 3.7 kcal/mol.

(© Wiley-VCH Verlag GmbH & Co. KGaA, 69451 Weinheim, Germany, 2005)

Introduction

The chemistry of aluminum complexes containing the bulky 3,5-di-*tert*-butylpyrazolato ($t\text{Bu}_2\text{pz}$) ligand has been an active area of research over the past several years.^[1–4] Advances that have emerged from this work include the first examples of η^2 -pyrazolato ligand coordination to a group 13 element,^[2,3c] structural models for ligand species that occur in alumoxanes,^[3b,3g] new coordination modes for acetylide groups,^[3d,3f] as well as stabilization of bridging alkyl and hydride groups in pyrazolate-bridged dimers.^[4] Roesky has reported the synthesis of the complex $[\text{H}_2\text{Al}(\mu:\eta^1,\eta^1\text{-}t\text{Bu}_2\text{pz})_2\text{AlH}_2]$, which was obtained by treatment of equimolar amounts of alane–trimethylamine with

$t\text{Bu}_2\text{pzH}$,^[3f] and has also described many reactions of this complex.^[3b,3d,3e,3g] As part of our work relating to the synthesis of aluminum complexes with bridging hydride ligands,^[4a] we have discovered a family of dimeric pyrazolato complexes that are derived from the reaction of alane–ethyltrimethylamine with $t\text{Bu}_2\text{pzH}$ in a 2:3 stoichiometry. These complexes are of the general formula $[(\eta^2\text{-}t\text{Bu}_2\text{pz})\text{AlH}(\mu:\eta^1,\eta^1\text{-}t\text{Bu}_2\text{pz})_2\text{Al}(\text{X})\text{H}]$, where X = H, OH, or $\eta^1\text{-}t\text{Bu}_2\text{pz}$. In addition to providing additional rare examples of structurally characterized group 13 complexes containing η^2 -pyrazolato ligands, this work describes the first crystal structure of a complex containing η^1 -, η^2 -, and $\mu:\eta^1,\eta^1$ -pyrazolato ligands as well as a structurally characterized aluminum complex containing a terminal hydroxo ligand. Aluminum complexes containing terminal hydroxo ligands are very rare,^[5] and have been of significant recent interest as models for species that might be present in methylalumoxanes used in olefin polymerization processes.^[5,6] The terminal hydroxoaluminum ligand described herein is stabilized by formation of an intramolecular hydrogen bond to the π -cloud of an adjacent pyrazolato ligand, which constitutes a novel hydrogen bonding interaction for a terminal hydroxo complex.

^[a] Department of Chemistry, Wayne State University, Detroit, Michigan 48202, USA
Fax: (internat.) + 1-313-577-8289
E-mail: chw@chem.wayne.edu

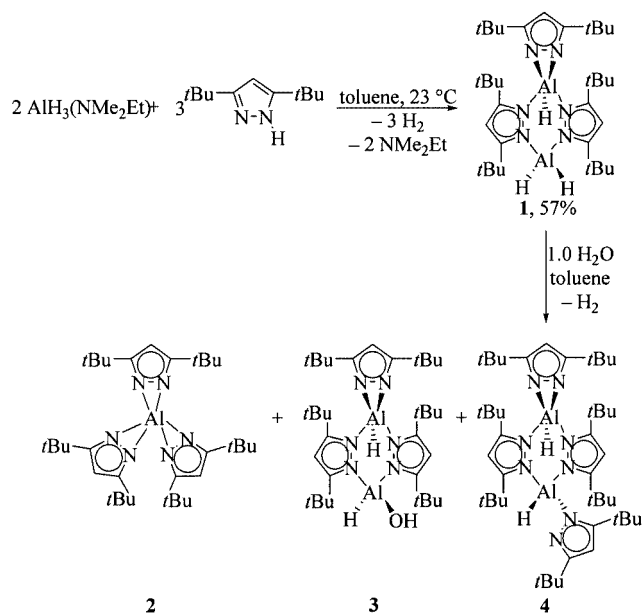
^[‡] Current address: Dalian Institute of Chemical Physics, Chinese Academy of Sciences, 457 Zhongshan Road, Dalian, Liaoning 116023, P. R. China

^[††] Current address: Sigma–Aldrich Corporation, 5485 County Rd. V, Sheboygan, Wisconsin 53085, USA

Results

Synthetic Chemistry

Scheme 1 outlines the synthetic approaches to the complexes that were prepared in this study. Treatment of alane–ethyltrimethylamine with $t\text{Bu}_2\text{pzH}$ in a 2:3 stoichiometry led to the dimeric pyrazolato complex **1** in 57% crystallized yield. ^1H NMR spectroscopic analysis of the reaction product demonstrated that **1** was the only product formed, when extreme care was taken to exclude water from the reaction. The structure of **1** is proposed based upon spectral and analytical data and from correlation with the structurally characterized hydrolysis products **3** and **4** described below.



Scheme 1. Preparation and hydrolysis of **1**

In the ^1H NMR spectrum of **1** in $[\text{D}_8]\text{toluene}$ at $-90\text{ }^\circ\text{C}$, the *tert*-butyl methyl groups appear as three equal intensity singlets at $\delta = 1.73$, 1.43 , and 1.22 ppm. The hydride resonances are observed as 1:1:1 intensity broad singlets at $\delta = 6.1$, 5.4 , and 3.3 ppm, and the pyrazolato CH groups appear as singlets at $\delta = 6.32$ and 6.20 ppm in a 1:2 ratio. The infrared spectrum shows the Al–H absorptions at 1962 , 1905 , and 1890 cm^{-1} . It was discovered that extended standing (> 1 week) of a hexane solution at $23\text{ }^\circ\text{C}$ led to the slow decomposition of **1** to $t\text{Bu}_2\text{pzH}$, **2**, and new compounds. As described below, the new compounds were obtained as pure materials and identified to be **3** and **4** from the hydrolysis of **1**.

Treatment of **1** with water (1 equiv.) at $-78\text{ }^\circ\text{C}$ in toluene led to immediate gas evolution and the formation of a white, insoluble precipitate. Workup of the reaction mixture, followed by fractional crystallization from hexane, afforded pure samples of **2** (8%), **3** (15%), and **4** (23%) as colorless crystalline solids. The identity of **2** was confirmed by comparison of its ^1H and $^{13}\text{C}\{^1\text{H}\}$ NMR spectra with

those previously reported by Deacon.^[2] The formulations of **3** and **4** were based upon their spectral and analytical data, and from their X-ray crystal structures as described below. The ^1H NMR spectrum of **3** in $[\text{D}_8]\text{toluene}$ at ambient temperature showed resonances for one type of pyrazolato ligand, implying that exchange between the $\mu\text{:}\eta^1,\eta^1\text{-}$ and the $\eta^2\text{-}$ pyrazolato ligands is faster than the NMR timescale. Upon cooling to $-60\text{ }^\circ\text{C}$, three equal intensity singlets for the *tert*-butyl methyl groups are observed at $\delta = 1.47$, 1.43 , and 1.18 ppm and the pyrazolato methine resonances appear as a broad singlet at $\delta = 6.22$ ppm. In addition, extremely broad resonances are observed at $\delta = 5.5$ and 4.4 ppm in a 1:2 ratio, which correspond to some combination of the Al–H and Al–OH fragments. The low temperature ^1H NMR spectrum of **3** is very similar to that of **1** and indicates similar structures. The infrared spectrum of **3** shows a strong hydroxy stretch at 3227 cm^{-1} and aluminum–hydrogen stretches at 1961 , 1908 , and 1860 cm^{-1} . The low position of the hydroxy stretch is consistent with hydrogen bonding, yet there is no evidence in the crystal structure for dihydrogen bonding or intermolecular hydrogen bonding. Instead, it is likely that the hydroxy hydrogen atom is intramolecularly hydrogen-bonded to the π -cloud of the adjacent $\eta^2\text{-}$ pyrazolato ligand. This possibility is explored below in more detail using molecular orbital calculations. The ^1H NMR spectra of **4** show little difference at room temperature and $-80\text{ }^\circ\text{C}$, and reveal two equal intensity pyrazolato ligands. These data are consistent with slow exchange between the $\mu\text{:}\eta^1,\eta^1\text{-}$ pyrazolato ligands and the $\eta^1\text{-}$ and $\eta^2\text{-}$ pyrazolato ligand sites, but with rapid exchange between the $\eta^1\text{-}$ and $\eta^2\text{-}$ pyrazolato ligand sites. The infrared spectrum of **4** shows an aluminum–hydrogen stretch at 1937 cm^{-1} .

The yield of **3** could be increased to 45% in a one-pot reaction of alane–ethyltrimethylamine with 3,5-di-*tert*-butylpyrazole in a 2:3 ratio, followed by addition of water (1 equiv.), stirring for 2 h, workup, and then fractional crystallization from hexane. Attempts to increase the yield of **4** did not meet with much success. Treatment of alane–ethyltrimethylamine with $t\text{Bu}_2\text{pzH}$ in a 2:4 ratio, followed by workup, afforded a crude product consisting of **2** (68%), **3** (24%), and **4** (8%).

X-ray Crystal Structures of **3** and **4**

Complexes **3** and **4** were characterized by X-ray crystallography in order to understand their three dimensional structures. The molecular structures of **3** and **4** are shown in Figures 1 and 2, respectively. The crystal data are given in Table 1.

Complex **3** consists of a dinuclear unit in a boat conformation held together by two $\mu\text{:}\eta^1,\eta^1\text{-}t\text{Bu}_2\text{pz}$ ligands. One aluminum center is bonded to $\eta^2\text{-}t\text{Bu}_2\text{pz}$ and hydride ligands, while the other aluminum atom is bonded to hydroxo and hydride ligands. The hydroxo and $\eta^2\text{-}$ pyrazolato ligands are *syn* to each other within the dimer. The aluminum–nitrogen bond lengths to five-coordinate Al(1) range between $1.936\text{--}1.968\text{ \AA}$, and are slightly shorter for four-coordinate Al(2) [$1.914(3)$, $1.920(3)\text{ \AA}$]. The

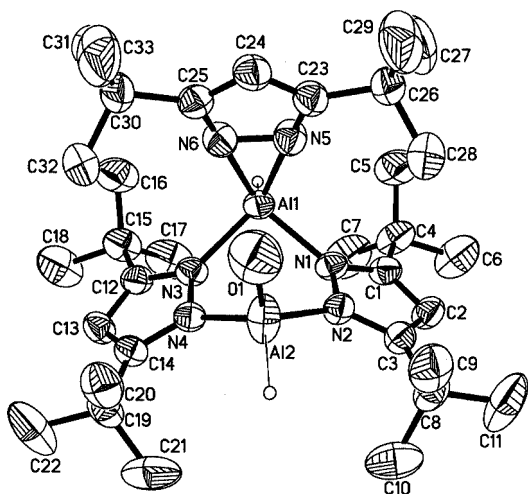


Figure 1. Perspective view of **3** with thermal ellipsoids at the 50% probability level

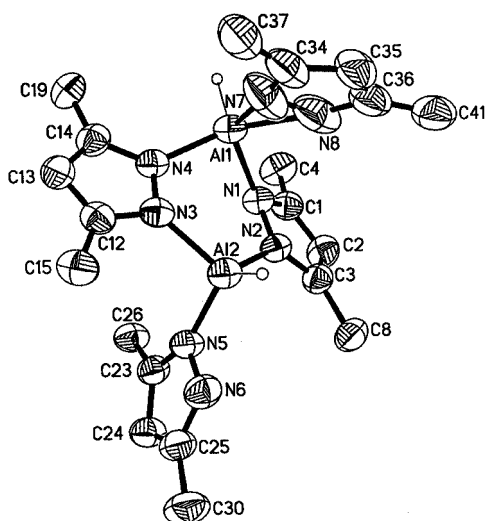


Figure 2. Perspective view of **4** with thermal ellipsoids at the 50% probability level; the *tert*-butyl methyl groups have been omitted for clarity

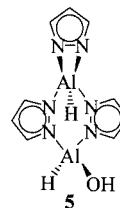
aluminum–oxygen bond length is 1.867(3) Å. The μ : η^1 , η^1 -pyrazolato ligands place the aluminum centers far enough apart [Al(1)–Al(2) 3.289(2) Å], so that hydrogen or oxygen atoms do not bridge in **3**. The N(5)–Al(1)–N(6) angle is 42.32(11)°, which is typical of η^2 -pyrazolato ligands bonded to aluminum.^[2,3c] All intermolecular OH...H(hydride) contacts are > 6 Å, and the closest intermolecular OH...O contact is > 4.3 Å. Thus, intermolecular dihydrogen bonding or intermolecular hydrogen bonding in **3** can be ruled out. The low hydroxy stretch noted above in the infrared spectrum of **3**, however, may be due to intramolecular hydrogen bonding between the hydroxy hydrogen atom and the π -cloud of the η^2 -pyrazolato ligand (OH...centroid distance = 2.574 Å).

The molecular structure of **4** is similar to that of **3** except that it contains an η^1 -*t*Bu₂pz ligand instead of a hydroxo ligand on the four-coordinate aluminum atom. The η^1 - and

η^2 -pyrazolato ligands are *anti* to each other within the dinuclear unit to minimize steric interactions. The non-bridging pyrazolato ligand planes are nearly perpendicular to each other due to the steric hindrance of the *tert*-butyl groups. The five-coordinate Al(1)–N bond lengths range between 1.892–2.082 Å, and are slightly longer than those of the four-coordinate Al(2)–N bonds (1.871–1.933 Å). The Al(1)–N(7) bond length [1.892(3) Å] is much shorter than the Al(1)–N(8) bond length [2.082(4) Å], indicating unsymmetrical coordination of the η^2 -pyrazolato ligand.^[3c,7] The Al(2)–N(6) distance is 2.559(3) Å, which clearly demonstrates η^1 -coordination. The N(7)–Al(1)–N(8) angle is 40.55(13)°, which is slightly smaller than the value in **3**. The Al(1)–Al(2) distance is 3.414(2) Å, which is slightly longer than in **3**, possibly due to increased steric crowding in **4**. Additionally, the intramolecular hydrogen bond in **3** may serve to reduce the aluminum–aluminum distance.

Molecular Orbital Calculations of **3**

To gain better insight into the nature of the pyrazolato ligand bonding and the intramolecular hydrogen bond in **3**, molecular orbital calculations were performed. All calculations were carried out using the Gaussian suite of programs.^[8] First we studied the model system **5**, in which the *tert*-butyl groups on the pyrazolato ligands were replaced by hydrogen atoms. Previous work from our laboratories indicated that replacement of alkyl groups by hydrogen atoms in pyrazolato ligands does not significantly affect the electronic structure of the molecule.^[9] Optimization of **5** at the B3LYP/6-311++G(d,p) level of theory^[10–13] led to the transformation of the η^2 -pz ligand in **5** to an η^1 -pz ligand. In addition, the π -cloud of the η^1 -pyrazolato ligand twisted away from the hydroxy group hydrogen atom on the adjacent Al atom. Hence, **5** was not an acceptable theoretical model for **3**, which suggested that the bulky *tert*-butyl groups on the pyrazolato ligands in **3** may play an important role in determining the overall structure.



We next sought to carry out molecular orbital calculations on the full experimental molecule **3**. Since **3** has a large number of atoms, an ONIOM approach was employed to reduce the cost of the overall calculation.^[14] The high level portion of **3** was the same as the model system and was calculated by B3LYP/6-311++G(d,p). The *tert*-butyl groups on the pyrazolato ligands were included in the low-level portion and were calculated by the AM1 semi-empirical method.^[15,16] Figure 3 presents the results of this treatment. Optimization of **3** afforded a less dramatic movement of the η^2 -pyrazolato ligand to the η^1 -bonding mode

Table 1. Summary of crystallographic data for **3** and **4**

| | 3 | 4 |
|--|--|---|
| Empirical formula | C ₃₃ H ₆₀ Al ₂ N ₆ O | C ₄₄ H ₇₈ Al ₂ N ₈ |
| Formula mass | 610.83 | 773.10 |
| Temp. [K] | 295(2) | 295(2) |
| Crystal system | Triclinic | Triclinic |
| Space group | <i>P</i> $\bar{1}$ | <i>P</i> $\bar{1}$ |
| <i>a</i> [Å] | 11.7811(11) | 9.9494(14) |
| <i>b</i> [Å] | 13.1426(13) | 11.7026(16) |
| <i>c</i> [Å] | 14.6042(14) | 21.031(3) |
| α [°] | 63.993(2) | 93.582(3) |
| β [°] | 83.503(3) | 90.742(3) |
| γ [°] | 68.072(2) | 90.646(4) |
| <i>V</i> [Å ³] | 1881.8(3) | 2442.5(6) |
| <i>Z</i> | 2 | 2 |
| <i>D</i> _{calcd.} [g/cm ³] | 1.078 | 1.051 |
| Abs coeff [mm ⁻¹] | 0.109 | 0.096 |
| <i>F</i> (000) | 668 | 848 |
| Cryst size [mm] | 0.35 × 0.20 × 0.12 | 0.20 × 0.20 × 0.15 |
| θ range [°] | 1.83 to 28.32 | 1.94 to 28.30 |
| Index ranges | -14 ≤ <i>h</i> ≤ 15 -15 ≤ <i>k</i> ≤ 16 0 ≤ <i>l</i> ≤ 19 | -12 ≤ <i>h</i> ≤ 12 -15 ≤ <i>k</i> ≤ 15 0 ≤ <i>l</i> ≤ 27 |
| No. of reflections collected | 13657 | 17562 |
| No. of independent reflections | 8616 (<i>R</i> _{int} = 0.035) | 11119 (<i>R</i> _{int} = 0.040) |
| No. of data/restraints/parameters | 8616/0/406 | 11119/0/536 |
| GOF/ <i>F</i> ² | 0.837 | 0.820 |
| <i>R</i> indices [<i>I</i> > 2σ(<i>I</i>)] | <i>R</i> ₁ = 0.0621 | <i>R</i> ₁ = 0.0605 |
| <i>wR</i> ₂ = 0.1519 | <i>wR</i> ₂ = 0.1448 | |
| <i>R</i> indices (all data) | <i>R</i> ₁ = 0.1822 | <i>R</i> ₁ = 0.1957 |
| <i>wR</i> ₂ = 0.1853 | <i>wR</i> ₂ = 0.1837 | |
| Largest diff peak/hole [e ⁻ Å ⁻³] | 0.264/-0.622 | 0.574/-0.252 |

$$R(F) = \frac{\sum ||F_o| - |F_c||}{\sum |F_o|}; R_w(F) = \frac{[\sum w(F_o^2 - F_c^2)^2 / \sum w(F_o^2)]^{1/2}}$$

(Figure 3, a). The computed aluminum–nitrogen bond lengths were 1.89 Å and 2.43 Å, compared to 1.96 Å determined experimentally for both bonds. A constrained system was optimized in which the aluminum–nitrogen bonds were fixed at the experimentally observed distances. This treatment led to an energy increase of only 1.4 kcal/mol (Figure 3, c), and subsequent unconstrained optimization of this system afforded the structure shown in Figure 3 (a). This small energy difference indicates that the stabilization for the η^2 -configuration is within the energy of crystal packing, and suggests that the η^2 -*t*-Bu₂pz ligand in **3** originates due to accommodation of the bulky *tert*-butyl groups. In both cases it is evident that there is an intramolecular hydrogen bond. In the fixed bond structure (Figure 3, c), the range of distances for the hydroxy hydrogen atom to the atoms in the pyrazolato ring core is 2.68–3.18 Å. In the case where the aluminum–nitrogen bond lengths were not frozen (Figure 3, a), these numbers have a slightly higher range of 2.61–3.56 Å. To obtain an estimate of the stabilization energy resulting from the hydrogen bond, the hydrogen atom on the hydroxy group was turned away from the pyrazolato ligand so that the hydroxy hydrogen atom was not in the proximity of the π -cloud of the η^2 -pyrazolato ligand (Figure 3, b). The optimized geometry for this system had aluminum–nitrogen bond lengths of 1.88 Å and 2.32 Å. The distances from the oxygen atom of the hydroxo

ligand to the atoms in the adjacent pyrazolato ligand ranged from 3.72–5.11 Å. Removing the ability to hydrogen bond from the system led to an ONIOM energy increase of 3.7 kcal/mol. This may be a slight underestimate of the true bond strength due to some steric differences in the low-level portion of the ONIOM calculation.

Discussion

The significance of this work resides principally in the unusual structures of **3** and **4**. Complex **4** is the first species that contains η^1 -, η^2 -, and μ : η^1 , η^1 -pyrazolato ligands within a single molecule. Many pyrazolato complexes have been reported that contain two of these coordination modes,^[1,3b,17] but none until now has contained all three. Aluminum complexes containing η^2 -pyrazolato ligands remain extremely rare,^[2,3c] so **3** and **4** are additionally novel from this perspective.

Complex **3** is a rare example of an aluminum compound that contains a terminal hydroxo ligand.^[18] The first structurally characterized aluminum complexes containing terminal hydroxo ligands were reported in 1987.^[5d,5e] A terminal hydroxo ligand was structurally documented in [Al₄Si₄H₈O₂₀·24H₂O]⁴⁻, and has a hydroxoaluminum–oxygen bond length of 1.783 Å.^[5d] Each hydroxo ligand is extensively hydrogen-bonded to interstitial water molecules.

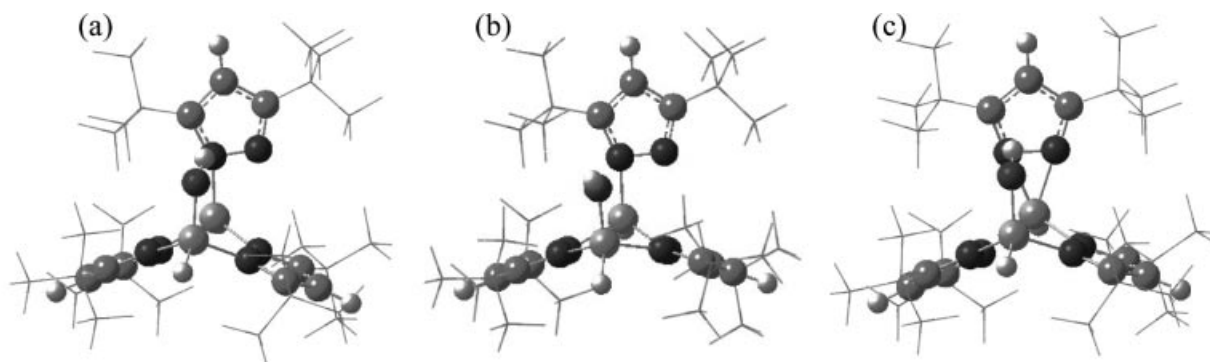


Figure 3. The three configurations of the model system with the DFT contribution as ball-and-stick and the AM1 portion as line drawing; (a) model system with intramolecular hydrogen bond; (b) model system with hydroxy group reversed so there is no intramolecular hydrogen bond; (c) model system with the aluminum–nitrogen bond lengths constrained to experimental values

The other initial report described the structure of quinuclidinium hydroxo(2,2',2''-nitrilotriphenoxy)aluminate, which contains an anionic aluminum center bonded to a terminal hydroxo ligand.^[5c] The quinuclidinium ion is also associated with the oxygen atom through a N–H···O hydrogen bond. The aluminum–oxygen bond length is 1.765(2) Å. Recently, Roesky and co-workers have reported a series of aluminum complexes containing terminal hydroxo ligands.^[5a–5c,18] The complexes are of the formula $L_{Ar}Al(OH)_2$,^[5a] $\{L_{Ar}Al(OH)\}_2(\mu-O)$,^[5b] and $L_{Ar}Al(OH)OAl(L_{Ar})(OCH=NtBu)$,^[5c] where $L_{Ar} = HC\{(CMe)(2,6-iPr_2C_6H_3N)\}_2$. The aluminum–oxygen bond lengths in $L_{Ar}Al(OH)_2$ are 1.6947(15) and 1.7107(16) Å.^[5a] In the solid state, this molecule forms dimeric units with $Al_2O_4H_2$ rings that contain intramolecular Al–O–H···O(H)(Al) hydrogen bonds. $\{L_{Ar}Al(OH)\}_2(\mu-O)$ exists as a monomer in the solid state, with aluminum–oxygen bond lengths of 1.738(2) and 1.741(3) Å.^[5b] Infrared spectroscopy suggests that the hydroxy groups do not participate in hydrogen bonding. It was proposed that the hydroxo ligand hydrogen atoms reside within the shielding cone of the L_{Ar} aromatic rings, due to an unusually upfield resonance for these hydrogen atoms ($\delta = -0.30$ ppm). $L_{Ar}Al(OH)OAl(L_{Ar})(OCH=NtBu)$ exists in the solid state with an eight-membered Al_2CHNO_3 ring that includes a strong O–H···N hydrogen bond.^[5c] The aluminum–oxygen bond length is 1.727(2) Å. Parkin reported the synthesis of $[HB(Me_2pz)_3]Al(OH)_2$ in 1990, although this complex was not structurally characterized and it is therefore not clear if it contains terminal hydroxo ligands.^[5f]

The metrics and stabilization of the terminal hydroxo ligand in **3** can be compared with those of the previously reported terminal hydroxo complexes noted above. The aluminum–oxygen bond length in **3** is 1.867(3) Å, which is considerably longer than the values in related terminal hydroxo complexes. However, the aluminum–oxygen bond length in **3** is similar to values observed in recently reported aluminum complexes containing bridging hydroxo ligands (1.81–2.09 Å).^[19] The hydroxo ligand hydrogen atom in **3** participates in hydrogen bonding to the π -cloud of the adjacent η^2 -pyrazolato ligand within the dimer, and thus

constitutes a unique coordination environment for the hydroxo ligand. Apparently, the *t*Bu₂pz ligands in **3** are so bulky that intermolecular hydrogen or dihydrogen bonding is not possible, and the only hydrogen-bond donor available is the π -cloud of the adjacent η^2 -pyrazolato ligand. To the best of our knowledge, this is the first example of a hydrogen bond to the π -cloud of a pyrazolato ligand. Hydrogen bonding between nitrogen–hydrogen and oxygen–hydrogen bonds and the π -clouds of various neutral aromatic compounds is well precedented.^[20] Since the *t*Bu₂pz ligand is aromatic and possibly more electron rich than a neutral aromatic compound due to the formal negative charge, its π -system is probably a good hydrogen-bond acceptor. Molecular orbital calculations suggest that there is a preference for the formation of the O–H···pz π hydrogen bond, and that an estimate of the bond strength for this interaction is about 3.7 kcal/mol. This bond strength is in the range of a typical weak hydrogen bond, but is enough to orient the hydroxo ligand hydrogen atom. Molecular orbital calculations suggest that there is a very small energy difference (1.4 kcal/mol) between η^1 - and η^2 -pyrazolato ligands in **3**. It is possible that the hydrogen bond in **3** helps to stabilize the η^2 -pyrazolato ligand, since the molecular orbital calculations suggested that there may be stronger hydrogen bonding to this ligand coordination mode compared to the η^1 -pyrazolato ligand mode. The hydrogen bond in **3** requires that the hydroxo ligand hydrogen atom is pointed directly at the shielding cone of the aromatic *t*Bu₂pz ligand. Thus, the ¹H NMR chemical shift of this hydrogen atom should be considerably upfield of where it would appear in the absence of this interaction. There is some ambiguity regarding the assignment of this resonance in **3**, since it appears in the same region as the aluminum-bound hydrido ligands. However, it resonates in the region of $\delta = 4.6$ –5.5 ppm. For comparison, the ¹H NMR chemical shift of the hydroxo ligand protons in $L_{Ar}Al(OH)_2$ was $\delta = 12.47$ ppm.^[5a] In $\{L_{Ar}Al(OH)\}_2(\mu-O)$, where it was proposed that the hydroxo ligand protons reside within the shielding cone of the L_{Ar} aromatic rings, the hydroxo proton resonance appeared at $\delta = -0.30$ ppm.^[5c] Roesky has argued that terminal Al–OH protons are strong Brønsted

acids, and should resonate at low fields in the ^1H NMR spectra in the absence of other effects.^[5a] This speculation supports the low field position of the hydroxo ligand resonance in $\text{L}_{\text{Ar}}\text{Al}(\text{OH})_2$. The hydroxo ligand resonance in **3** is considerably upfield of that in $\text{L}_{\text{Ar}}\text{Al}(\text{OH})_2$, and therefore may be shifted due to the interaction with the shielding cone of the pyrazolato π -cloud.

Complex **3** is relevant to alumoxane chemistry,^[12] since terminal hydroxo ligands may be present in some alumoxanes and the acidic hydroxo ligand hydrogen atom may activate polymerization precatalysts through protonation of a metal–alkyl bond. The existence of **3** must be related to the presence of the extremely bulky $t\text{Bu}_2\text{pz}$ ligands, which block further reactions such as protonation of hydrido or pyrazolato ligands. The stabilization of terminal hydroxo ligands in the previously reported aluminum complexes^[5] is generally achieved only in the presence of very bulky ancillary ligands, which can block further reactions. Thus, terminal hydroxo ligands, if they occur in methylalumoxanes, probably occupy extremely hindered sites. The high Brønsted acidity of the aluminum-bound hydroxo ligand proton leads to a strong preference for hydrogen bond formation. As noted above, most of the known terminal hydroxo complexes of aluminum are stabilized by hydrogen bonding and have unique hydrogen-bond acceptors. The only exception is $\{\text{L}_{\text{Ar}}\text{Al}(\text{OH})\}_2(\mu\text{-O})$, for which infrared spectroscopy suggested a non-hydrogen-bonded hydroxo ligand. In **3**, we have documented the presence of unique intramolecular $\text{O}\cdots\text{H}\cdots\text{pz}\pi$ hydrogen bonding.

Experimental Section

General: All reactions were performed under dry argon using standard Schlenk and dry-box techniques. Solvents were distilled from various drying agents under argon prior to use. Alane–ethyltrimethylamine was purchased from commercial sources. 3,5-Di-*tert*-butylpyrazole was prepared according to a literature procedure.^[21] ^1H and $^{13}\text{C}\{^1\text{H}\}$ NMR spectra were obtained in dry, degassed $[\text{D}_8]\text{toluene}$, and were referenced to the residual proton or carbon atom resonances of this solvent. Infrared spectra were obtained using Nujol as the medium. Elemental analyses were performed by Midwest Microlab, Indianapolis, IN. Melting points were obtained on a Haake-Buchler HBI digital melting point apparatus and are uncorrected.

Synthesis of 1: A 100-mL Schlenk flask was charged with a 0.5 M solution of $\text{AlH}_3(\text{NMe}_2\text{Et})$ in toluene (6.0 mL, 3.0 mmol) and was further diluted with toluene (40 mL). $t\text{Bu}_2\text{pzH}$ (0.811 g, 4.5 mmol) was added to this solution at 23 °C in small portions over 0.25 h. The mixture was stirred at 23 °C for 16 h. At this point, the volatile components were removed under reduced pressure to afford a white solid. This solid was dissolved in hexane (30 mL) and the solution was filtered through a 2-cm pad of Celite on a coarse glass frit. The filtered solution was placed in a -20 °C freezer for 24 h, during which time crystallization occurred. Removal of the solvent by cannula, followed by vacuum drying, afforded **1** as colorless crystals (0.505 g, 57%); m.p. 110 °C (dec). IR (Nujol): $\tilde{\nu}_{\text{AlH}}$ = 1961 (m), 1906 (m), 1885 (m) cm^{-1} . ^1H NMR ($[\text{D}_8]\text{toluene}$, 23 °C): δ = 1.40 [s, 54 H, $\text{C}(\text{CH}_3)_3$], 4.5 (br. s, 3 H, Al–H), 6.16 (s, 3 H, pz C–H) ppm. $^{13}\text{C}\{^1\text{H}\}$ NMR ($[\text{D}_8]\text{toluene}$, 23 °C): δ = 31.00 [s, $\text{C}(\text{CH}_3)_3$],

32.44 [s, $\text{C}(\text{CH}_3)_3$], 103.49 (s, pz C–H), 164.37 [s, C– $\text{C}(\text{CH}_3)_3$] ppm. $\text{C}_{33}\text{H}_{60}\text{Al}_2\text{N}_6$ (594.84): calcd. C 66.63, H 10.17, N 14.13; found C 66.84, H 10.10, N 13.95.

Hydrolysis of 1 to Afford 2, 3, and 4: A 100-mL Schlenk flask containing a solution of **1** (0.479 g, 0.805 mmol) in toluene (20 mL) was treated with water (14.5 mg, 0.805 mmol) at -78 °C. Gas evolution was immediately noted and small amount of insoluble white material precipitated. The mixture was stirred at -78 °C for 3 h and was then warmed to ambient temperature and was further stirred for 15 h. The volatile components were then removed under reduced pressure to afford a white solid. Dissolution of this solid in hexane (20 mL), followed by filtration through a 2-cm pad of Celite on a coarse glass frit to remove a small amount of insoluble white solid, afforded a colorless solution. Fractional crystallization of this solution at -20 °C afforded colorless crystals of **2** (0.035 g, 7.7%), **3** (0.075 g, 15%), and **4** (0.145 g, 23%). The order of crystallization was **3**, **2**, and **4**. The isolated yields were diminished due to the care that was required to achieve pure samples. NMR spectroscopic analysis of the white solid removed by filtration showed it to contain $t\text{Bu}_2\text{pzH}$ as well as a solid that was insoluble in $[\text{D}_1]\text{chloroform}$.

Complex 2: This compound was identified by comparison of its ^1H and ^{13}C NMR chemical shifts with the reported values.^[2]

Data for 3: M.p. 145 °C. IR (Nujol): $\tilde{\nu}$ = 3227 (s, ν_{AlOH}), 1961 (m, ν_{AlH}), 1908 (m, ν_{AlH}), 1860 (m, ν_{AlH}) cm^{-1} . ^1H NMR ($[\text{D}_8]\text{toluene}$, 23 °C): δ = 1.41 [s, 54 H, $\text{C}(\text{CH}_3)_3$], 5.5, 4.6 (2 br. s, 3 H, 2 Al–H, Al–OH), 6.16 (s, 3 H, pz C–H) ppm. $^{13}\text{C}\{^1\text{H}\}$ NMR ($[\text{D}_8]\text{toluene}$, 23 °C): δ = 31.14 [s, $\text{C}(\text{CH}_3)_3$], 32.58 [s, $\text{C}(\text{CH}_3)_3$], 103.61 (s, pz C–H), 164.55 (s, C– $\text{C}(\text{CH}_3)_3$) ppm. $\text{C}_{33}\text{H}_{60}\text{Al}_2\text{N}_6\text{O}$ (610.83): calcd. C 64.87, H 9.90, N 13.76; found C 64.59, H 9.76, N 13.94.

Data for 4: M.p. 135 °C (dec). IR (Nujol): $\tilde{\nu}$ = 1937 (w, ν_{AlH}) cm^{-1} . ^1H NMR ($[\text{D}_8]\text{toluene}$, 23 °C): δ = 1.12 (s, 36 H, 4 $\text{C}(\text{CH}_3)_3$), 1.41 (s, 36 H, 4 $\text{C}(\text{CH}_3)_3$), 4.9 (br. s, 2 H, Al–H), 6.02 (s, 2 H, pz C–H), 6.22 (s, 2 H, pz C–H) ppm. $^{13}\text{C}\{^1\text{H}\}$ NMR ($[\text{D}_8]\text{toluene}$, 23 °C): δ = 31.00 [s, $\text{C}(\text{CH}_3)_3$], 31.39 [s, $\text{C}(\text{CH}_3)_3$], 31.94 [s, $\text{C}(\text{CH}_3)_3$], 33.31 [s, $\text{C}(\text{CH}_3)_3$], 101.12 (s, pz C–H), 106.93 (s, pz C–H), 162.12 [s, C– $\text{C}(\text{CH}_3)_3$], 168.69 [s, C– $\text{C}(\text{CH}_3)_3$] ppm. $\text{C}_{44}\text{H}_{78}\text{Al}_2\text{N}_8$ (773.10): calcd. C 68.36, H 10.17, N 14.49; found C 68.22, H 10.10, N 14.27.

X-ray Crystallography: Crystals of **3** ($M = 610.83$) and **4** ($M = 773.10$) were grown as described above and crystallized in the triclinic crystal system in the space group $\text{P}\bar{1}$. Relevant details and data are summarized in Tables 1–3. The crystals were mounted in thin glass capillaries under nitrogen. Diffraction data were collected with a Bruker P4 four-circle diffractometer coupled to a Bruker CCD area detector at 295(2) K, with graphite-monochromated Mo- K_α radiation ($\lambda = 0.71073$ Å). The structures were solved from the Patterson maps using SHELX-97^[22] and refined against F^2 on all data by full-matrix least-squares with the same program. All non-hydrogen atoms were refined anisotropically. The hydrogen atoms were included in the model at their geometrically calculated positions and held riding or observed on a difference fourier and refined. CCDC-185702 (**3**) and -185701 (**4**) contain the supplementary crystallographic data for this paper. These data can be obtained free of charge on application to CCDC, 12 Union Road, Cambridge CB21EZ, UK [Fax: (internat.) + 44-1223-336-033; E-mail: deposit@ccdc.cam.ac.uk]. Structure searches were conducted using the Cambridge Crystallographic Database, Version 5.25, November 2003.

Table 2. Selected distances [Å] and angles [°] for 3

| | |
|---|------------|
| Al(1)–N(1) | 1.964(3) |
| Al(1)–N(5) | 1.936(3) |
| Al(1)–N(6) | 1.954(3) |
| Al(2)–N(2) | 1.920(3) |
| Al(2)–N(4) | 1.914(3) |
| Al(2)–O(1) | 1.867(3) |
| Al(1)–H(1) | 1.423(5) |
| Al(2)–H(2) | 1.534(5) |
| H(O1)⋯centroid[η ² -pz] | 2.574 |
| Al(1)⋯Al(2) | 3.289(2) |
| N(1)–Al(1)–N(3) | 95.11(11) |
| N(5)–Al(1)–N(6) | 42.32(11) |
| N(2)–Al(2)–N(4) | 102.64(11) |
| N(2)–Al(2)–O(1) | 119.45(14) |
| N(4)–Al(2)–O(1) | 115.19(15) |
| O(1)–H(O1)–centroid(η ² -pz) | 152.9 |

Table 3. Selected distances [Å] and angles [°] for 4

| | |
|-----------------|------------|
| Al(1)–N(1) | 1.947(3) |
| Al(1)–N(4) | 1.952(3) |
| Al(1)–N(7) | 1.892(3) |
| Al(1)–N(8) | 2.082(4) |
| Al(2)–N(2) | 1.922(3) |
| Al(2)–N(3) | 1.933(3) |
| Al(2)–N(5) | 1.871(3) |
| Al(2)–N(6) | 2.559(3) |
| Al(1)–H | 1.521(5) |
| Al(2)–H | 1.453(5) |
| Al(1)⋯Al(2) | 3.414(2) |
| N(1)–Al(1)–N(4) | 96.45(11) |
| N(1)–Al(1)–N(7) | 123.90(16) |
| N(1)–Al(1)–N(8) | 91.57(14) |
| N(7)–Al(1)–N(8) | 40.55(13) |
| N(2)–Al(2)–N(3) | 109.12(12) |
| N(2)–Al(2)–N(5) | 104.28(11) |
| N(3)–Al(2)–N(5) | 105.63(11) |

Acknowledgments

C. H. W. and H. B. S. thank the U.S. National Science Foundation for support of this research (C. H. W.: Grant Nos. CHE-9807269, Special Creativity Extension thereto, CHE-0314615; H. B. S.: Grant No. CHE-0131157). J. E. K. thanks the Wayne State University Institute for Scientific Computing for support provided by an NSF-IGERT Fellowship.

- [1] For reviews of pyrazolato complexes, see: [1^a] A. P. Sadimenko, *Adv. Heterocyclic Chem.* **2001**, *80*, 157–240. [1^b] J. E. Cosgriff, G. B. Deacon, *Angew. Chem. Int. Ed.* **1998**, *37*, 286–287; *Angew. Chem.* **1998**, *110*, 298–299. [1^c] G. La Monica, G. A. Arduozzo, *Progr. Inorg. Chem.* **1997**, *46*, 151–238. [1^d] A. P. Sadimenko, S. S. Basson, *Coord. Chem. Rev.* **1996**, *147*, 247–297. [1^e] S. Trofimenko, *Progr. Inorg. Chem.* **1986**, *34*, 115–210. [1^f] S. Trofimenko, *Chem. Rev.* **1972**, *72*, 497–508.
- [2] G. B. Deacon, E. E. Delbridge, C. M. Forsyth, P. C. Junk, B. W. Skelton, A. H. White, *Aust. J. Chem.* **1999**, *52*, 733–739.
- [3] [3^a] W. Zheng, H. W. Roesky, N. C. Mösch-Zanetti, H.-G. Schmidt, M. Noltemeyer, *Eur. J. Inorg. Chem.* **2002**, 1056–1059. [3^b] W. Zheng, H. W. Roesky, M. Noltemeyer, *Organometallics* **2001**, *20*, 1033–1035. [3^c] W. Zheng, N. C. Mösch-Zanetti, T. Blunck, H. W. Roesky, M. Noltemeyer, H.

- G. Schmidt, *Organometallics* **2001**, *20*, 3299–3303. [3^d] W. Zheng, H. Hohmeister, N. C. Mösch-Zanetti, H. W. Roesky, M. Noltemeyer, H.-G. Schmidt, *Inorg. Chem.* **2001**, *40*, 2363–2367. [3^e] W. Zheng, A. Stasch, J. Prust, H. W. Roesky, F. Cimpoesu, M. Noltemeyer, H.-G. Schmidt, *Angew. Chem. Int. Ed.* **2001**, *40*, 3461–3464; *Angew. Chem.* **2001**, *113*, 3569–3572. [3^f] W. Zheng, N. C. Mösch-Zanetti, H. W. Roesky, M. Hewitt, F. Cimpoesu, T. R. Schneider, A. Stasch, J. Prust, *Angew. Chem. Int. Ed.* **2000**, *39*, 3099–3101; *Angew. Chem.* **2000**, *112*, 3229–3231. [3^g] W. Zheng, N. C. Mösch-Zanetti, H. W. Roesky, M. Noltemeyer, M. Hewitt, H.-G. Schmidt, T. R. Schneider, *Angew. Chem. Int. Ed.* **2000**, *39*, 4276–4279; *Angew. Chem.* **2000**, *112*, 4446–4449.
- [4] [4^a] Z. K. Yu, J. M. Wittbrodt, A. Xia, M. J. Heeg, H. B. Schlegel, C. H. Winter, *Organometallics* **2001**, *20*, 4301–4303. [4^b] Z. K. Yu, M. J. Heeg, C. H. Winter, *Chem. Commun.* **2001**, 353–354. [4^c] Z. K. Yu, J. M. Wittbrodt, M. J. Heeg, H. B. Schlegel, C. H. Winter, *J. Am. Chem. Soc.* **2000**, *122*, 9338–9339.
- [5] [5^a] Y. Peng, G. Bai, H. Fan, D. Vidovic, H. W. Roesky, J. Magull, *Inorg. Chem.* **2004**, *43*, 1217–1219. [5^b] G. Bai, H. W. Roesky, J. Li, M. Noltemeyer, H.-G. Schmidt, *Angew. Chem. Int. Ed.* **2003**, *42*, 5502–5506. [5^c] G. Bai, Y. Peng, H. W. Roesky, J. Li, H.-G. Schmidt, M. Noltemeyer, *Angew. Chem. Int. Ed.* **2003**, *42*, 1132–1135. [5^d] I. Smolin, Y. F. Shepelev, A. S. Ershov, D. Khobbel, *Dokl. Akad. Nauk SSSR* **1987**, *297*, 1377. [5^e] E. Muller, H.-B. Bürgi, *Helv. Chim. Acta* **1987**, *70*, 520–533. [5^f] A. Looney, G. Parkin, *Polyhedron* **1990**, *9*, 265–276.
- [6] For selected leading reviews of alumoxanes, see: [6^a] E. Y.-X. Chen, T. J. Marks, *Chem. Rev.* **2000**, *100*, 1391–1434. [6^b] H. W. Roesky, M. G. Walawalkar, R. Murugavel, *Acc. Chem. Res.* **2001**, *34*, 201–211. [6^c] S. Pasykiewicz, *Polyhedron* **1990**, *9*, 429–453.
- [7] For other examples of slipped η²-pyrazolato ligands, see: [7^a] I. A. Guzei, G. P. A. Yap, C. H. Winter, *Inorg. Chem.* **1997**, *36*, 1738–1739. [7^b] G. B. Deacon, E. E. Delbridge, C. M. Forsyth, B. W. Skelton, A. H. White, *J. Chem. Soc., Dalton Trans.* **2000**, 745–754.
- [8] Gaussian 01 (Development Version): M. J. Frisch, G. W. Trucks, H. B. Schlegel, G. E. Scuseria, M. A. Robb, J. R. Cheeseman, J. A. Montgomery Jr., T. Vreven, K. N. Kudin, J. C. Burant, J. M. Millam, S. S. Iyengar, J. Tomasi, V. Barone, B. Mennucci, M. Cossi, G. Scalmani, N. Rega, G. A. Petersson, H. Nakatsuji, M. Hada, M. Ehara, K. Toyota, R. Fukuda, J. Hasegawa, M. Ishida, T. Nakajima, H. Honda, O. Kitao, H. Nakai, M. Klene, X. Li, J. E. Knox, H. P. Hratchian, J. B. Cross, C. Adamo, J. Jaramillo, R. Gomperts, R. E. Stratmann, O. Yazyev, A. J. Austin, R. Cammi, C. Pomelli, J. W. Ochterski, P. Y. Ayala, K. Morokuma, G. A. Voth, P. Salvador, J. J. Dannenberg, V. G. Zakrzewski, S. Dapprich, A. D. Daniels, M. C. Strain, O. Farkas, D. K. Malick, A. D. Rabuck, K. Raghavachari, J. B. Foresman, J. V. Ortiz, Q. Cui, A. G. Baboul, S. Clifford, J. Cioslowski, B. B. Stefanov, G. Liu, A. Liashenko, P. Piskorz, I. Komaromi, R. L. Martin, D. J. Fox, T. Keith, M. A. Al-Laham, C. Y. Peng, A. Nanayakkara, M. Challacombe, P. M. W. Gill, B. Johnson, W. Chen, M. W. Wong, C. Gonzalez, J. A. Pople, Gaussian Inc., Pittsburgh, PA, **2002**.
- [9] I. A. Guzei, A. G. Baboul, G. P. A. Yap, A. L. Rheingold, H. B. Schlegel, C. H. Winter, *J. Am. Chem. Soc.* **1997**, *119*, 3387–3388.
- [10] A. D. Becke, *J. Chem. Phys.* **1993**, *98*, 5648–5652.
- [11] A. D. Becke, *Phys. Rev. A* **1988**, *38*, 3098–3100.
- [12] C. Lee, W. Yang, R. D. Parr, *Phys. Rev. B* **1988**, *37*, 785–789.
- [13] A. D. McLean, G. S. Chandler, *J. Chem. Phys.* **1980**, *72*, 5639.
- [14] S. Dapprich, I. Komaromi, K. S. Byun, K. Morokuma, M. J. Frisch, *Theochem – J. Mol. Struct.* **1999**, *462*, 1–21.
- [15] M. J. S. Dewar, E. G. Zoebisch, E. F. Healy, J. J. P. Stewart, *J. Am. Chem. Soc.* **1985**, *107*, 3902–3909.
- [16] M. J. S. Dewar, A. J. Holder, *Organometallics* **1990**, *9*, 508–511.
- [17] For selected recent examples of pyrazolato complexes contain-

- ing two distinct coordination modes, see: ^[17a] G. B. Deacon, A. Gitlits, B. W. Skelton, A. H. White, *Chem. Commun.* **1999**, 1213–1214. ^[17b] G. A. Aridizzoia, G. La Monica, A. Maspero, N. Masciocchi, M. Moret, *Eur. J. Inorg. Chem.* **1999**, 1301–1307. ^[17c] G. B. Deacon, E. E. Delbridge, B. W. Skelton, A. H. White, *Angew. Chem. Int. Ed.* **1998**, *37*, 2251–2252; *Angew. Chem.* **1998**, *110*, 2372–2373. ^[17d] D. Carmona, F. J. Lahoz, L. A. Oro, M. P. Lamata, S. Buzarra, *Organometallics* **1991**, *10*, 3123–3131. ^[17e] M. K. Ehlert, S. J. Rettig, A. Storr, R. C. Thompson, J. Trotter, *Can. J. Chem.* **1990**, *68*, 1494–1498. ^[17f] H. Schumann, P. R. Lee, J. Loebel, *Angew. Chem. Int. Ed. Engl.* **1989**, *28*, 1033–1035; *Angew. Chem.* **1989**, *101*, 1073–1075. ^[17g] L. A. Oro, D. Carmona, M. P. Lamata, C. Foces-Foces, F. H. Cano, *Inorg. Chim. Acta* **1985**, *97*, 19–23.
- ^[18] For a recent overview, see: H. W. Roesky, R. Murugavel, M. R. Walawalkar, *Chem. Eur. J.* **2004**, *10*, 324–331.
- ^[19] For selected examples of structurally characterized aluminum complexes containing bridging hydroxo ligands [Al–O 1.81–2.09 Å], see: ^[19a] P. Wei, D.A. Atwood, *Polyhedron* **1999**, *18*, 641–646. ^[19b] J. Storre, A. Klemp, H. W. Roesky, H.-G. Schmidt, M. Noltemeyer, R. Fleischer, D. Stalke, *J. Am. Chem. Soc.* **1996**, *118*, 1380–1386. ^[19c] R. J. Wehmschulte, W. J. Grigsby, B. Schiemenz, R. A. Bartlett, P. P. Power, *Inorg. Chem.* **1996**, *35*, 6694–6702. ^[19d] Y. Koide, A. R. Barron, *Organometallics* **1995**, *14*, 4026–4029. ^[19e] C. C. Landry, C. J. Harlan, S. G. Bott, A. R. Barron, *Angew. Chem. Int. Ed. Engl.* **1995**, *34*, 1201–1202; *Angew. Chem.* **1995**, *107*, 1315–1317. ^[19f] C. J. Harlan, M. R. Mason, A. R. Barron, *Organometallics* **1994**, *13*, 2957–2969. ^[19g] M. R. Mason, J. M. Smith, S. G. Bott, A. R. Barron, *J. Am. Chem. Soc.* **1993**, *115*, 4971–4984.
- ^[20] For leading references, see: ^[20a] M. A. Muñoz, O. Sama, M. Galán, P. Guardado, C. Carmona, M. Balón, *Spectrochim. Acta, Part A* **2001**, *57*, 1049–1054. ^[20b] V. Stefov, Lj. Pejov, B. Šoptrajanov, *J. Mol. Struct.* **2000**, *555*, 363–368. ^[20c] P. Ganis, A. Cecon, T. Köhler, F. Manoli, S. Santi, A. Venzo, *Inorg. Chem. Commun.* **1998**, *1*, 15–17. ^[20d] A. Nikolic, A. Petrovic, D. Antonovic, L. Gobor, *J. Mol. Struct.* **1997**, *408/409*, 355–359. ^[20e] F. D. Lewis, J.-S. Yang, C. L. Stern, *J. Am. Chem. Soc.* **1996**, *118*, 12029–12038. ^[20f] M. Crisma, F. Formaggio, G. Valle, C. Toniolo, M. Saviano, R. Iacovino, L. Zaccaro, E. Bendetti, *Biopolymers* **1997**, *42*, 1–8.
- ^[21] J. Elguéro, E. Gonzalez, R. Jacquier, *Bull. Soc. Chim. Fr.* **1968**, 707–709.
- ^[22] G. Sheldrick, University of Göttingen, Germany, **1997**.

Received July 28, 2004

Early View Article

Published Online November 18, 2004